Surface instabilities in crystal growth of dilute alloys

Alexander L. Korzhenevskii

Institute for Problems of Mechanical Engineering, RAS, Bol'shoi Prospekt V.O. 61, St. Petersburg 199178, Russia

Richard Bausch

Institut für Theoretische Physik IV, Heinrich-Heine-Universität Düsseldorf, Universitätsstrasse 1, D-40225 Düsseldorf, Germany

Rudi Schmitz

Institut für Theoretische Physik A, RWTH Aachen, Templergraben 55, D-52056 Aachen, Germany

In crystal growth of a dilute alloy from a melt, the way of spreading of solute atoms into the liquid and solid phases leads to a variety of dynamic instabilities of the crystal surface. In addition to the diffusion-induced Mullins-Sekerka instability, leading to dendritic structures, a couple of new instabilities is shown to appear due to the segregation of solute atoms in the interface region. Each of these instabilities occurs within a velocity window, which, controlled by the system parameters, appears like a new phase in a nonequilibrium situation.

The most fascinating nonequilibrium phenomenon in crystal growth from a melt is the spontaneous formation of dendritic or cellular patterns, extensively described in the classical review[1] by Langer. Such processes are initiated by instabilities of the solidification front, which, at low undercooling of the melt, are driven by heat or particle diffusion, as pointed out by Mullins and Sekerka.[2] The late-stage dendritic growth has been described in a remarkable analytic approach by Brener.[3]

At sufficiently large undercooling of the melt, a finite growth rate of the crystal develops, which, according to Misbah *et al.*,[4] leads to a change of the Mullins-Sekerka instability. The transition between this kinetic and diffusive regimes has been discussed by Löwen *et al.*[5] on the basis of a phase-field description. In the kinetics-controlled regime, they found, within a one-dimensional numerical calculation, the fragment of a new metastable behavior.

In the present Brief Report, we perform a three-dimensional stability analysis for a set of exactly treatable models of growing dilute alloys, where, as a common feature, the solute atoms are supposed to have a constant mobility in the melt but zero mobility in the solid. The procedure is similar to the simpler one in Ref. 6, which, with regard to internal domain boundaries, assumed a uniform overall mobility of the solute atoms. Our present analysis sheds some light on the metastable behavior, gleaming through in Ref. 5. More importantly, however, it predicts new instabilities due to the segregation of solute atoms at the crystal surface, which frequently occurs in multicomponent materials.[7]

The growth behavior of a dilute alloy in the z direction is most simply described by the equations of motion,

$$\partial_t Z = \beta \left(F - \frac{\delta H}{\delta Z} \right),$$

$$\partial_t C = \nabla B \nabla \frac{\delta H}{\delta C}, \qquad (1)$$

for the position $Z(\mathbf{x},t)$ of the crystal surface and for the excess density $C(\mathbf{r},t)$ of solute atoms relative to the crystal

phase. Here, β and $B(\mathbf{r},t)$ measure the mobility of the surface and of the solute atoms, respectively, and $F(\mathbf{x},t)$ is a driving force generated by undercooling the melt and restricted to imply $|\partial Z| \ll 1$. Furthermore,

$$H = \frac{\sigma}{2} \int d^2x (\partial Z)^2 + \frac{\kappa}{2} \int d^3r [C - U(z-Z)]^2 \qquad (2)$$

is an effective Hamiltonian, where σ means the surface tension of the crystal surface and $\kappa \equiv \partial\mu/\partial C$, involving the chemical potential μ of the solute component in the equilibrium state of the melt. The equilibrium condition $\delta H/\delta C = 0$ implies that $U(z-Z)$ is the density profile of the solute atoms in a local-equilibrium state.

This profile will, in general, invade the liquid and solid regions in different ways. Denoting its range on the solid side by ξ, we refine our definition of the excess density by assuming $U(z-Z)=0$ in the crystal phase $z < Z - \xi$. A major part of our analysis can be performed without any further specification of $U(z-Z)$. Since the mobility of the solute atoms is normally much smaller inside the crystal, we also assume $B(\mathbf{r},t)=(D/\kappa)\Theta[z-Z(\mathbf{x},t)+\xi]$, where D is the diffusion constant of the solute atoms in the liquid.

In favor of a transparent analysis, we now introduce dimensionless quantities by the scaling transformations $\tau\partial_t \to \partial_t, \lambda\nabla \to \nabla, Z/\lambda \to Z, \lambda^3 C \to C$, in which appropriate choices for basic length and time scales are $\lambda \equiv (\kappa/\sigma)^{1/5}$ and $\tau \equiv \lambda^2/D$. Then, in terms of the parameter $p \equiv \beta\sigma/D$, the equations of motion [Eq. (1)] assume the form

$$\partial_t Z = p[\partial^2 Z + F - (U', C - U)],$$

$$\partial_t C = \nabla^2 (C - U), \qquad (3)$$

for $z > Z - \xi$, where the scalar product (X, Y) means integration over z. The second equation in Eq. (3) is supplemented by the boundary condition $\partial_z(C-U)|_{z=Z-\xi}=0$, implied by our our assumption on $B(\mathbf{r},t)$, and by the condition $C(z=\infty)=0$, specifying the growth process.

In the case of a constant undercooling $F=\Delta-1$, a planar

crystal surface will move with constant velocity v in the z direction, joined by a stationary density profile of the form $C_v(z-vt) \equiv C_v(\zeta)$ in the comoving frame. The quantities v and $C_v(\zeta)$ then follow from the equations

$$v = p[\Delta - 1 + G + U^2(\infty)/2],$$

$$-vC_v = (C'_v - U'), \tag{4}$$

where the contribution

$$G(v) \equiv -(U', C_v) = -v(C_v, C_v) \tag{5}$$

acts as a solute-drag force. The second equation in Eq. (4) has the solution

$$C_v(\zeta) = \int_{-\xi}^{\zeta} d\eta\, U'(\eta) \exp[-v(\zeta - \eta)], \tag{6}$$

for $\zeta > -\xi$, whereas $C_v = 0$ in the crystal phase $\zeta < -\xi$.

In order to test the stability of the uniform growth process, we add to the driving force $\Delta - 1$ an extra term $f(\mathbf{x}, t)$, giving rise to increments $h(\mathbf{x}, t) \equiv Z(\mathbf{x}, t) - vt$ and $c(\mathbf{x}, \zeta, t) \equiv C(\mathbf{x}, \zeta, t) - C_v(\zeta) + C'_v(\zeta) h(\mathbf{x}, t)$. This implies, to lowest order of an expansion in ∂h,

$$\partial_t h = p[\partial^2 h + f + g],$$

$$\partial_t c = v\partial_\zeta c + (\partial_\zeta^2 + \partial^2)c + [U'\partial_t - vC_v(\partial_t - \partial^2)]h, \tag{7}$$

where we have introduced the local-drag force

$$g(\mathbf{x}, t) \equiv -(U', c)(\mathbf{x}, t). \tag{8}$$

Again, the second equation in Eq. (7) applies to the regime $\zeta > -\xi$, now with boundary conditions $\partial_\zeta c|_{\zeta = -\xi} = c(\infty) = 0$.

The first equation in Eq. (7) provides a formal expression for the response function $R(\mathbf{x}, t) \equiv \delta h(\mathbf{x}, t)/\delta f(0, 0)$. In terms of Fourier-Laplace transforms $\hat{R}(\mathbf{q}, s), \hat{h}(\mathbf{q}, s), \hat{c}(\mathbf{q}, \zeta, s)$, permitting the replacements $\partial \rightarrow i\mathbf{q}, \partial_t \rightarrow s$, we find

$$\hat{R}(\mathbf{q}, s) = \frac{1}{s/p + q^2 + \Sigma(\mathbf{q}, s)}, \tag{9}$$

where, according to Eq. (8), $\Sigma(\mathbf{q}, s) \equiv (U', \hat{c})(\mathbf{q}, s)/\hat{h}(\mathbf{q}, s)$. For an explicit evaluation of Eq. (9), we, therefore, need the solution of the second equation in Eq. (7), which is given by

$$\hat{c}(\mathbf{q}, \zeta, s) = \left\{ \frac{\alpha^2 - q^2}{v + 2\alpha} \left[C_{v+\alpha}(\zeta) - \bar{C}_\alpha(\zeta) \right. \right.$$

$$\left. - \frac{\alpha}{v + \alpha} \bar{C}_\alpha(-\xi) \exp[-(v + \alpha)(\zeta + \xi)] \right]$$

$$\left. + v[C_{v+\alpha}(\zeta) - C_v(\zeta)] \right\} \hat{h}(\mathbf{q}, s), \tag{10}$$

where $\alpha \equiv -(v/2) + \sqrt{(v/2)^2 + s + q^2}$, and

$$\bar{C}_\alpha(\zeta) \equiv -\int_\zeta^\infty d\eta\, U'(\eta) \exp[\alpha(\zeta - \eta)]. \tag{11}$$

We mention that the solution [Eq. (10)] only applies to the regime $\mathrm{Re}(s) + Dq^2 > 0$, where an instability might occur.
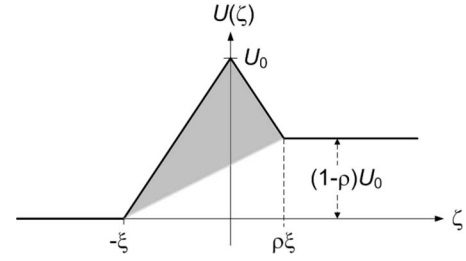

FIG. 1. The model potential $U(\zeta)$, showing a segregation peak at $\zeta = 0$, and a miscibility gap, given by $(1-\rho)U_0$. The shaded region of size $\rho\xi U_0$ represents the surface excess.

Pole singularities of $R(\mathbf{q}, s)$ correspond to branches of eigenmode frequencies of the system which conveniently characterize the instabilities of the crystal surface. Their properties are, therefore, summarized in the dispersion relation $1/R(\mathbf{q}, s) = 0$ or, more explicitly,

$$\frac{s}{p} + q^2 - v[G(v + \alpha) - G(v)]$$

$$= \frac{\alpha^2 - q^2}{v + 2\alpha} \left[G(v + \alpha) + G(\alpha) - \frac{\alpha}{v + \alpha} \bar{C}_\alpha(-\xi) \bar{C}_{v+\alpha}(-\xi) \right]. \tag{12}$$

This main result of our present investigation is exact, up to the restriction to lowest-order contributions in ∂h, which consistently matches the level of our basic model. Another remarkable feature, emphasizing the universal character of the result [Eq. (12)], is its independence on the details of the equilibrium profile $U(\zeta)$. This allows us to study a sequence of models with increasing complexity where in each extension, some new parameter appears, which generates a new type of surface instability.

The most general model profile, considered in the present Brief Report, is shown in Fig. 1. It has a segregation peak at the center $\zeta = 0$ which spreads out into the solid and liquid phases by distances ξ and $\rho\xi$, respectively. The surface excess, represented by the shaded region in Fig. 1, is given by $\Gamma \equiv \rho\xi U_0$ and the miscibility gap, also visible in Fig. 1, has the size $\Delta C = (1 - \rho)U_0$.

We initially adopt the sharp-interface approximation $\rho, \xi \rightarrow 0$, which implies $\bar{C}_v(0) = -U_0$ and $G = -U_0^2/2$. If these values are inserted in Eq. (12), one recovers the dispersion relation

$$(U_0^2 v - q^2 - s/p)(v + \alpha) = U_0^2(s + v^2), \tag{13}$$

derived previously by Misbah et al.[4] Simultaneously, the first equation in Eq. (4) reduces to $v = p(\Delta - 1)$, so that the limit $p \rightarrow \infty$ corresponds to the boundary $\Delta = 1$ of the diffusion-controlled regime, suggesting to add the quasistationary limit $v/q \rightarrow 0$. In this case, Eq. (13) reduces to the simplest form of the Mullins-Sekerka dispersion relation

$$s = qv[1 - q^2/(U_0^2 v)], \tag{14}$$

which only depends on U_0 and is known to describe a diffusion-induced instability of the crystal surface. In the

general case, p enters as a second parameter and, as shown in Ref. 4, leads to a new instability of kinetic origin in the velocity window $0 < v < v_0 \equiv U_0^2$.

The drag force, resulting for $\xi, \rho \neq 0$, is given by

$$G(v) = U_0^2 \{3 - (1 + \rho)\xi v + \exp[-(1 + \rho)\xi v]$$
$$- 2[\exp(-\xi v) + \exp(-\rho \xi v)]\}/(\xi v)^2. \quad (15)$$

In the dispersion relation [Eq. (12)], this leads to a nontrivial α dependence, which prevents a full analytic evaluation. Since, however, we are interested in the kinetic regime $\Delta > 1$, implying finite values of v, we expand Eq. (12) in α and finally in $s + q^2$. We then discover two branches $s = s_i(q)$ with the behavior $s_1(0) = s_1'(0) = s_2'(0) = 0$ which signal instabilities, if at least one of the quantities $s_1''(0), s_2(0)$ is positive. Independently of the form of the drag force, one obtains

$$s_1''(0) = 2\frac{G'(v) - [G(v) + G(0)]/v - 1}{1/p - G'(v)},$$

$$s_2(0) = 2\frac{1/p - G'(v)}{[G(v) + G(0)/v]''}, \quad (16)$$

where the denominator in the second line turns out to be negative in all cases of interest.

On the basis of the results [Eq. (16)], we now discuss the model, defined by Fig. 1, at $\rho = 0$. Then, the segregation peak in $U(\zeta)$ disappears, leaving a finite slope U_0/ξ in the transition region between the solid and liquid phases. This mimics the density profile, arising from standard phase-field models.[5] In the actual case, the numerator $N(v) \equiv G'(v) - [G(v) + G(0)]/v - 1$ in the first equation in Eq. (16) has the approximate form $N(v) \approx v_0/v - 1$ near $v = 0$ and is monotonously decreasing for $v > 0$. In the normal case $F'(v) \equiv 1/p - G'(v) > 0$, we thus recover the instability, known from Eq. (13). Since, however, $F'(0) = 1/p - 1/p_c$ with $p_c \equiv 6/(U_0^2 \xi)$, the anomalous behavior $F'(v) < 0$ will occur in the case $p > p_c$ within an interval $0 < v < v_2$, where $F'(v_2) = 0$. In fact, the behavior $F''(v) > 0$ for $v > 0$ ensures that v_2 is the only zero of $F'(v)$ and, in the small-velocity range, given by $v_2 \approx 2(1 - p_c/p)/\xi$. The surprising conclusion is that in the case $p > p_c$, the unstable regime of the mode $s_1(q)$ is shifted to one of the possible velocity windows $v_0 < v < v_2$ or $v_2 < v < v_0$. Simultaneously, another unexpected instability of the type $s_2(q)$ will emerge in the regime $0 < v < v_2$.

We finally explore the influence of a segregation peak in $U(\zeta)$ by allowing nonzero values of ρ in the interval $0 < \rho < 1$. An instability of the mode $s_2(q)$ can still survive, now, however, in a velocity window $v_1 < v < v_2$ which, at sufficiently high values of ρ, separates from the origin $v = 0$. The instability is related to the jerky-flow phenomenon, pointed out by Cahn[8] in the problem of grain-boundary migration, and has been analyzed, in a more general context, in Ref. 6.

A true segregation-induced instability of the crystal surface arises from the branch $s_1(q)$. In order to study it in an isolated form, we temporarily consider the case $F'(v) > 0$, which suppresses instabilities of the mode $s_2(q)$. It is suffi-
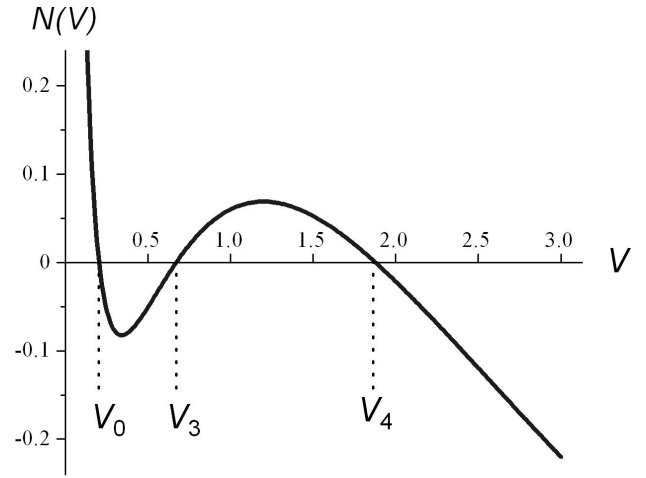

FIG. 2. The numerator of $s_1''(0)$, plotted as a function of the scaled velocity $V = v\xi$. The curve refers to the model potential of Fig. 1 at parameter values $W = U_0^2 \xi = 5.8$ and $\rho = 0.85$.

cient then to consider the form of $N(v)$, evaluated for the present case. In some part of the space, spanned by the parameters U_0, ξ, ρ, this function looks as shown in Fig. 2. Whereas $v_0 < v < v_3$ is a stable regime, a new instability appears in the velocity window $v_3 < v < v_4$. It is caused by convective flows of the solute atoms within the segregation layer which changes the local-drag force [Eq. (8)]. By suitably tuning the model parameters, it can be arranged that the maximum or the minimum in Fig. 2 hits the line $N(v) = 0$. These events mark transition points from zero to finite extent of the new stability and instability domains. More intricate arrangements of such domains arise in the temporarily disregarded case $F'(v) < 0$, which in the first equation in Eq. (16) inverts stable and unstable behaviors and via the second equation in Eq. (16) generates a new instability.

In the light of our results, we now comment on previous works on surface instabilities in the kinetics-controlled regime. Whereas our procedure confirms the conclusions for dilute alloys, derived in Ref. 4 within the sharp-interface approximation, our stability analysis for phase-field-like models complements the calculations in Ref. 5. These were restricted to one dimension but, nevertheless, indicate the appearance of a metastable regime for $p > p_c$. This fits well into the results of our predictions which hopefully can be checked by experiments. According to the table of material parameters in Ref. 5, appropriate candidates for experimental investigations are metallic alloys.

We finally want to discuss the possibilities to observe the new segregation-induced instability in experiments. This, in the first place, requires to estimate the values of the various velocity thresholds. As a benchmark, we first focus on the event where all zeros in Fig. 2 coincide, so that at this point $N(v_s) = N'(v_s) = N''(v_s) = 0$. These conditions fix the related value $\rho_s = 0.7962$, below which the segregation instability cannot occur. For the scaled quantities $V \equiv v\xi$ and $W \equiv U_0^2 \xi$, they also imply $V_s = 0.796$ and $W_s = 5.399$. In order to explore possible interferences with the anomalous behavior $F'(v) \leq 0$, we finally consider the critical point $F'(v_c) = F''(v_c) = 0$ at $\rho = \rho_s$, which yields $p/p_c = 0.171$ and $V_c = 3.9415$.

Since generally $V_0 < V_3 < V_s < V_4$ and $V_1 < V_c < V_2$, we will apply low-velocity approximations for V_0, V_1, V_3 and high-velocity approximations for V_2, V_4. The former case suggests to expand $G(v)$ in powers of v, which yields $V_0 \approx [6(1-\rho^2)/p_c], V_1 \approx [(4+p_c/p)/6], V_3 \approx (p_c/3)$ where in the latter two estimates we have assumed $\rho = 1$. At high velocities, we tentatively neglect the exponentials in Eq. (15), which implies $V_2 \approx V_4/2 \approx \sqrt{6/p_c}$.

As a final step, we now transform back all quantities, entering the velocity thresholds, to physical units. This does not affect the parameter p due to its definition and for velocities only requires to use the identity $V = v\xi/D$. An essential ingredient, however, is given by the result $p_c = [6\sigma\xi/(\partial\mu/\partial C)]/[(\Delta C)\xi + \Gamma]^2$, which generalizes the corresponding one in Ref. 5 to the case of nonzero surface excess. The physical expression $\Gamma = (\Delta C)\xi\rho/(1-\rho)$ arises from its dimensionless counterpart by splitting off a factor λ^2, reflecting the fact that this quantity strictly means the surface density of segregated solute particles. Some methods to determine the amount of the surface excess experimentally can be found in Ref. 7.

At sufficient strength of surface excesses, we expect, on the basis of our present investigation, that segregation-induced surface instabilities will generally occur in the growth of multicomponent materials. In such systems, they should influence dendritic growth processes and, even in the regime of rapid solidification, operate as new types of mechanisms for pattern formation. In the case of the anomaly $F'(v) < 0$, a variety of stability domains appears, which opens the opportunity to control the morphology of crystalline matter by tuning the system parameters.

We finally point out that, for internal defects with a symmetric equilibrium profile $U(z-Z)$ and a uniform diffusion constant D, the sharp-kink approximation and, consequently, the unstable branches [Eqs. (13) and (14)] do not exist. Furthermore, an instability of the type $F'(v) < 0$ then requires the presence of a segregation peak and, therefore, always comes along with a second segregation-induced instability. In contrast, instabilities of the type $F'(v) < 0$ occur in crystal growth even in the absence of a segregation peak. They are nevertheless completely ignored in most standard approaches, which we consider as an artifact of the sharp-kink approximation.

[1] J. S. Langer, Rev. Mod. Phys. **52**, 1 (1980).
[2] W. W. Mullins and R. F. Sekerka, J. Appl. Phys. **34**, 323 (1963).
[3] E. Brener, Phys. Rev. Lett. **71**, 3653 (1993).
[4] C. Misbah, H. Müller-Krumbhaar, and D. E. Temkin, J. Phys. I **1**, 585 (1991).
[5] H. Löwen, J. Bechhoefer, and L. S. Tuckerman, Phys. Rev. A **45**, 2399 (1992).
[6] A. L. Korzhenevskii, R. Bausch, and R. Schmitz, Phys. Rev. Lett. **97**, 176101 (2006).
[7] P. A. Dowben and A. Miller, *Surface Segregation Phenomena* (CRC, Boca Raton, FL, 1990).
[8] J. W. Cahn, Acta Metall. **10**, 789 (1962).